

## ARTICLES

**Density-functional study of the magnetic and metal-insulator transition of bcc hydrogen**

Bernd G. Pfommer and Steven G. Louie

*Department of Physics, University of California at Berkeley, Berkeley, California 94720  
and Materials Sciences Division, Lawrence Berkeley National Laboratory, Berkeley, California 94720*

(Received 20 July 1998)

A model body-centered cubic (bcc) hydrogen solid is studied using density functional theory in the local spin density approximation (LSDA) and in the generalized gradient approximation (GGA). In GGA, the paramagnetic to antiferromagnetic phase transition occurs at a higher density, and is in much better agreement with previous variational quantum Monte Carlo (VQMC) calculations than LSDA. The metal-insulator transition in GGA is observed at a higher density and is also closer to the VQMC result than LSDA. In the limit of isolated hydrogen atoms, we find that in GGA the self-consistent electron density is greatly improved over LSDA due to a better cancellation of the electronic self-interaction. [S0163-1829(98)06343-7]

**I. INTRODUCTION**

Although density functional theory (DFT) in the local spin density approximation (LSDA) correctly describes the electronic structure of many systems, it fails in certain cases. In particular, the typical Mott insulators such as the transition metal oxides FeO and CoO are found to be metals. For CuO, not even the antiferromagnetic (AFM) order, a ground state property, is reproduced.<sup>1</sup> Likewise, the undoped parent compound of high- $T_c$  materials  $\text{La}_2\text{CuO}_4$  is a paramagnetic metal<sup>2</sup> in LSDA, but an AFM insulator in experiment.

To overcome these difficulties, the LSDA has been improved in several different ways. The self-interaction-corrected (SIC) LSDA correctly predicts that MnO, FeO, CoO, NiO, and CuO are AFM insulators, and drastically improves gaps and local magnetic moments.<sup>3</sup> Due to the numerical effort involved, this method is, however, not readily applicable to larger systems.

Other studies employ a ‘‘LDA+ $U$ ’’ approach,<sup>1,2,4–6</sup> where the local density approximation (LDA) or LSDA are augmented by additional terms to introduce the Hubbard energy  $U$ . These methods have enjoyed considerable success<sup>2,5</sup> in that they correctly reproduce the AFM ground states of NiO, CoO, FeO, and  $\text{La}_2\text{CuO}_4$ . A systematic improvement of the ground-state and single-electron excited-state properties over LSDA has also been reported<sup>7</sup> for  $\text{LaMO}_3$  perovskites ( $M=\text{Ti-Cu}$ ). On the other hand, the method fails for early  $3d$  transition-metal oxides.<sup>1</sup>

Finally, generalized gradient approximations<sup>8</sup> (GGA) have been applied to Mott insulators. A fairly clear picture emerges from a literature review.<sup>9–12</sup> GGA systematically improves over LSDA, but often not enough. For instance, the insulating  $\text{YTiO}_3$  is metallic<sup>9</sup> both in GGA and LSDA, but with a smaller band overlap in GGA. GGA slightly enhances the magnetic moments of MnO, NiO, and CoO, and substantially improves the HOMO-LUMO band gaps of MnO and NiO.<sup>10</sup> In GGA, the AFM insulator  $\text{CaCuO}_2$  is found<sup>11</sup> to be a paramagnetic (PM) metal, but it is closer to an AFM insta-

bility than in LSDA. For  $\text{FeF}_2$ ,  $\text{CoF}_2$ ,<sup>11</sup>  $\text{YVO}_3$ , and  $\text{LaVO}_3$ ,<sup>12</sup> GGA correctly yields an insulator, whereas LSDA predicts a metal.

In this article, we compare the Ceperley-Alder<sup>13</sup> LSDA functional in the parametrization of Perdew and Zunger<sup>14</sup> with the Perdew-Wang 91 GGA functional (GGA PW91).<sup>8</sup> We consider two systems: atomic hydrogen and a model body-centered cubic (bcc) atomic hydrogen crystal. For atomic hydrogen, the exact solution to the electronic structure problem is known. In the bcc model solid, we can judge the quality of the density functionals by comparing with variational quantum Monte Carlo (VQMC) calculations from Zhu’s dissertation.<sup>15</sup> We will focus on the accuracy with which the density functionals reproduce the magnetic and the Mott metal-insulator transitions. This transition is of particular interest because of the ongoing experimental efforts to produce metallic hydrogen.<sup>16–18</sup> In contrast with many metal oxides, solid hydrogen is a rather delocalized system, since near the phase transition, the hydrogen  $1s$  wave functions overlap considerably. Therefore, the ‘‘LDA+ $U$ ’’ method might not be appropriate here.<sup>4</sup>

**II. HYDROGEN ATOM**

In the Kohn-Sham<sup>19</sup> approach, the electronic energy  $E_{\text{tot}}$  is the sum of four terms:

$$E_{\text{tot}} = T + V + E_H + E_{\text{xc}}. \quad (1)$$

For a single-electron system such as the hydrogen atom, the exchange-correlation energy  $E_{\text{xc}}$  should exactly cancel the spurious self-interaction Hartree energy  $E_H$ , such that only the kinetic energy  $T$  and the ionic potential energy  $V$  are left, and the corresponding Kohn-Sham equation turns into Schrödinger’s equation. The exchange-correlation energy  $E_{\text{xc}}$  can be decomposed further into exchange and correlation energy,  $E_{\text{xc}} = E_x + E_c$ , where  $E_x$  is defined as the Kohn-Sham exchange energy computed from the single-particle

TABLE I. Values (in Rydbergs) for total energy  $E_{\text{tot}}$ , kinetic energy  $T$ , potential energy  $V$ , Hartree energy  $E_H$ , exchange energy  $E_x$ , correlation energy  $E_c$ , and exchange-correlation energy  $E_{\text{xc}}$ . A self-consistent electron density is used for the GGA PW91 functional and the LSDA.

	$E_{\text{tot}}$	$T$	$V$	$E_H$	$E_x$	$E_c$	$E_{\text{xc}}$
Exact	-1	1	-2	0.625	-0.625	0	-0.625
LSDA	-0.958	0.933	-1.891	0.597	-0.513	-0.044	-0.557
PW91	-1.003	0.993	-1.991	0.615	-0.606	-0.013	-0.619

density matrix of the exact Kohn-Sham orbitals.<sup>20</sup> Obviously,  $E_x = -E_H$ , and therefore  $E_c = 0$ .

In Table I, we show the numerical values for the various terms in Eq. (1) for the hydrogen atom. The energies have been calculated with the self-consistent electron number densities  $n(\mathbf{r})$ . Similar results have been published previously,<sup>20,21</sup> but not for self-consistent densities. For comparison, we also show the exact analytic results in Table I. The GGA PW91 functional not only gives a much better agreement for the total energy than LSDA, but also the individual terms are closer to the exact values. Further, the separation between exchange and correlation appears to be improved, although from a practical point of view, this is immaterial.

As is evident from the kinetic and potential energy terms in Table I, the self-consistent electron densities in GGA PW91 and LSDA must differ. They are shown in Fig. 1, along with the exact density. We see that the GGA PW91 pulls the wave function in towards the nucleus, compared to the LSDA, such that the self-consistent density is much closer to the exact one. This also explains why the kinetic energy is higher, and the potential energy is lower in GGA PW91 than in LSDA.

The differences in the self-consistent electron density are due to the exchange-correlation potential  $v_{\text{xc}}(\mathbf{r}) = \delta E_{\text{xc}} / \delta n(\mathbf{r})$ . Figure 2 shows the exchange-correlation potentials for LSDA and GGA PW91, and the exact exchange-

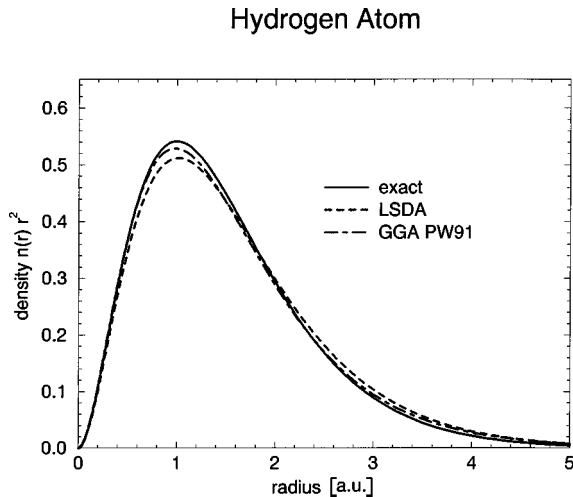


FIG. 1. Electron number density  $n(r)$  of the hydrogen atom as a function of the radius. Shown are the exact density (solid line), and the self-consistent densities in LSDA (dashed line) and GGA PW91 (dot-dashed line).

## Hydrogen Atom

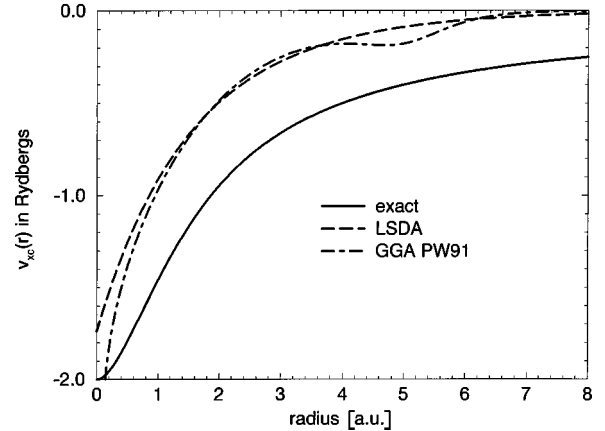


FIG. 2. Exchange-correlation potential  $v_{\text{xc}}(r)$  in Rydbergs for the hydrogen atom as a function of the radius. Shown are the exact  $v_{\text{xc}}$  (solid line), and the self-consistent  $v_{\text{xc}}$  in LSDA (dashed line) and GGA PW91 (dot-dashed line).

correlation potential, which is just the negative of the Hartree potential,  $v_H(\mathbf{r}) = \int [n(\mathbf{r}')/|\mathbf{r}-\mathbf{r}'|]d^3r'$ , using Rydberg units. We see that neither LSDA nor GGA PW91 track the exact exchange correlation potential well, and they both do not show the correct asymptotic limit<sup>22</sup> for large  $r$ , which is  $\lim_{r \rightarrow \infty} v_{\text{xc}}(r) = -2/r$ . The wiggle in the GGA PW91 exchange-correlation potential at about  $r=5$  a.u. (1 a.u. being the Bohr radius) is not an artifact of the numerical implementation, but stems from the particular functional form of the PW91 exchange potential. Notice also the divergence at the origin, which is intrinsic to all gradient-corrected functionals. The improved quality of the electron density in GGA PW91 over LSDA thus appears somewhat fortuitous, since the potential shows deficiencies at large and small  $r$ , but has just the appropriate slope in the regime between  $r \approx 1-3$  a.u. to yield a good density. A similar shape for  $v_{\text{xc}}(r)$ , and a comparable improvement of the self-consistent density has been previously reported for the closed-shell helium<sup>23</sup> and neon<sup>24</sup> atoms.

## III. SOLID HYDROGEN

A crystal of sufficiently separated hydrogen atoms obviously is an insulator. However, without magnetic order, a one-electron band structure picture predicts metallic behavior, because the  $1s$  band is only half filled. This error is remedied if AFM order is assumed,<sup>25</sup> which leads to a doubling of the unit cell size, and can open a band gap. With now two atoms in the unit cell, there are four bands derived from the atomic  $1s$  states (one for each spin and atom). Although by symmetry spin up and spin down bands are degenerate, the four bands can split into two pairs, separated by an energy gap. If the hydrogen atoms are brought closer together, the band dispersion increases, and at some critical lattice constant the occupied and unoccupied bands start overlapping, at which point the insulator becomes a metal. This can occur while still the AFM order is preserved. As the distance between the hydrogen atoms is decreased further, the AFM order vanishes, and a PM metal is found.

In contrast with the band theory of “itinerant” Bloch

electrons is the Hubbard model Hamiltonian approach,<sup>26</sup> which was developed to describe systems where the electrons are fairly localized. There, two parameters describe the physical properties of the system: the electron hopping interaction  $t$  and the intra-atomic Coulomb correlation interaction energy  $U$ . Except for a few special cases, exact solutions of the Hubbard model Hamiltonian are not known. Some important conclusions, however, can be drawn from it.<sup>27</sup> For instance, Hubbard<sup>26</sup> demonstrated that the existence of an insulating gap does not require spin order. This is quite in contrast to the Slater picture, where the insulating phase must be spin ordered. Based on a screening argument, Mott argued that the metal-insulator transition should be of first order, and suggested that the magnetic transition might occur simultaneously with the metal-insulator transition.<sup>28</sup> However, since the long-range Coulomb interaction is treated as a short-range phenomenon in the Hubbard model, the physics of the Hubbard model metal-insulator transition should be quite different<sup>27</sup> from the one originally suggested by Mott.<sup>29</sup>

By using the Kohn-Sham equations of DFT, we commit to band theory. There is no reason to believe that DFT must therefore fail. In fact, the magnetization is a ground state property, and is hence accessible to DFT. The Kohn-Sham eigenvalues on the other hand cannot be interpreted as quasiparticle excitation energies. It has been argued<sup>1</sup> that the gap in LSDA is related to a Hund's rule exchange term rather than the Hubbard parameter  $U$ , and therefore the gap will necessarily come out too small. Because Kohn-Sham eigenvalues are nevertheless frequently used to characterize materials, we will compare LSDA and GGA gaps with those obtained from VQMC calculations.

Several DFT studies of atomic hydrogen solids can be found in the literature.<sup>3,30-34</sup> Using LSDA and the linearized muffin-tin orbital method in the atomic sphere approximation (LMTO-ASA), Min *et al.*<sup>32</sup> report a PM-AFM transition for bcc hydrogen at a Wigner-Seitz radius of  $r_s = 2.55$  a.u., and a metal-insulator transition at  $r_s = 2.85$  a.u.. Moruzzi and Marcus<sup>33</sup> employ LSDA to study a hydrogen fcc lattice, where they find a second-order PM-FM transition at  $r_s = 2.7$  a.u. (the AFM solution was not considered). At  $r_s = 3.0$  a.u. they observe a second-order metal-insulator transition. Finally, Svane and Gunnarsson<sup>3</sup> compare LSDA with the self-interaction corrected LSDA (SIC-LSDA), and find SIC-LSDA to produce a simultaneous first order PM-AFM and metal-insulator transition at  $r_s = 2.45$  a.u. for the bcc hydrogen solid.

Our calculations on bcc hydrogen are performed using a local pseudopotential of the Kerker type<sup>35</sup> with a cutoff radius of 0.7 a.u. The wave functions are expanded in plane waves up to a 60 Ry energy cutoff. A  $14 \times 14 \times 14$  Monkhorst-Pack<sup>36</sup> grid is used to sample the Brillouin zone with 84  $k$  points in the irreducible wedge.

The results for the sublattice magnetic moment are shown in Fig. 3. In LSDA, the PM-AFM transition is found at  $r_s = 2.5$  a.u., in agreement with previous results.<sup>3,32</sup> With the GGA PW91, the phase transition occurs at the higher density  $r_s = 2.25$  a.u., which is much closer to the VQMC result of  $r_s = 2.2$  a.u. Thus, GGA not only improves the description of the hydrogen atom, but also of the solid. From the absence of hysteresis and the shape of the curves in Fig. 3, we conclude that the PM-AFM transitions in both LSDA and GGA PW91 are of second order, or at most very weakly first order. The

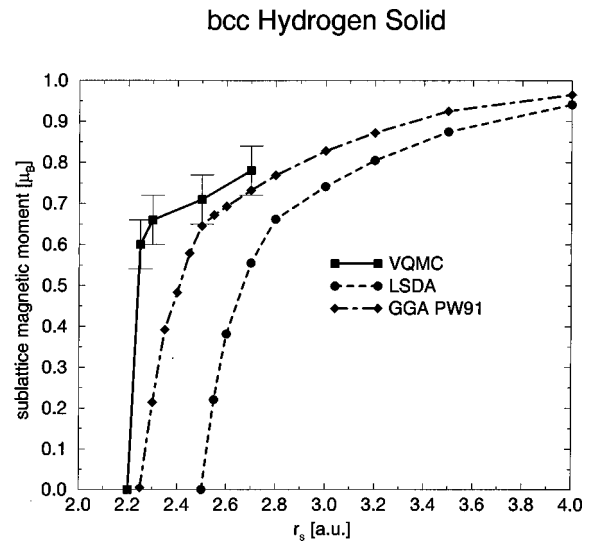


FIG. 3. Sublattice magnetic moment of the bcc atomic hydrogen solid in units of  $\mu_B$  (Bohr magneton) as a function of  $r_s$  in a.u. The GGA magnetic moment (dot-dashed line) is close to the VQMC result (solid line), and clearly improves over LSDA (dashed line).

VQMC results indicate a weak first-order transition,<sup>15</sup> but the statistical noise is too large for a definite statement. Notice that SIC-LSDA<sup>3</sup> observes the magnetic transition at  $r_s = 2.45$  a.u., although this value might not be reliable due to sensitivities to the LSDA functional parametrization.<sup>3</sup>

Figure 4 shows the band gap of bcc hydrogen at different densities. In close agreement with Min *et al.*,<sup>32</sup> we find bcc hydrogen to be an insulator in LSDA for  $r_s > 2.8$  a.u. Using GGA PW91, the metal-insulator transition is observed at  $r_s = 2.5$  a.u., and consequently occurs at lower density than the magnetic transition. VQMC on the other hand indicates metallic behavior for  $r_s$  smaller than about 2.2–2.3 a.u., and thus the Mott and PM-AFM transitions occur at very similar densities. The agreement between GGA and VQMC is not as good as for the magnetic transition, but is much improved over LSDA.

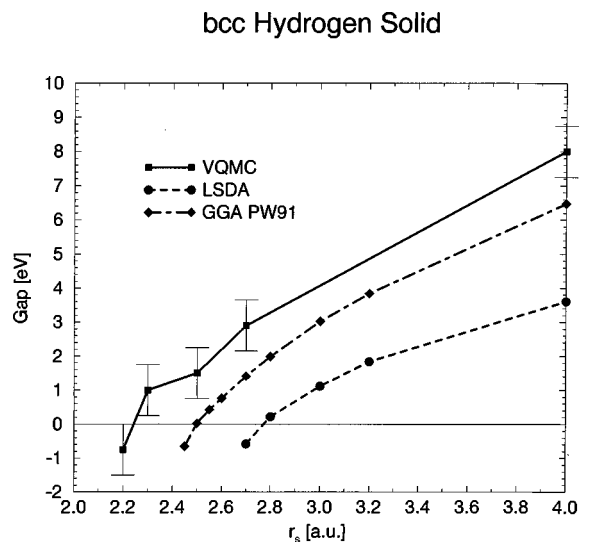


FIG. 4. Energy gap (in eV) of the bcc hydrogen solid as a function of  $r_s$  (in a.u.). The GGA gap (dot-dashed line) opens at lower densities than in LSDA (dashed line), but is still off from the VQMC result (solid line).

## IV. CONCLUSION

In conclusion, it has been shown that for a bcc hydrogen crystal, GGA gives a metal-insulator and a PM-AFM phase transition at higher density than LSDA, and is in better agreement with VQMC results. Both transitions are most likely of second order in both LSDA and GGA. In the limit of the isolated hydrogen atom, the better cancellation of the self-interaction Hartree term in GGA leads to an improved self-consistent electron density, although the exchange-correlation potential in GGA is rather different from the exact one.

## ACKNOWLEDGMENTS

B.P. would like to thank Dr. Jing Zhu and Dr. Angel Rubio for useful discussions. This work was supported by the NSF under Grant No. DMR-9520554, and by the Office of Energy Research, Office of Basic Energy Sciences, Materials Sciences Division of the U.S. Department of Energy under Contract No. DE-AC03-76SF00098. Computer time was provided by the NSF at the National Center for Supercomputing Applications and by the U.S. DOE at the Lawrence Berkeley National Laboratory's NERSC center.

- 
- <sup>1</sup>V. I. Anisimov, J. Zaanen, and O. K. Andersen, Phys. Rev. B **44**, 943 (1991).
- <sup>2</sup>M. Czyżyk and G. Sawatzky, Phys. Rev. B **49**, 14 211 (1994).
- <sup>3</sup>A. Svane and O. Gunnarsson, Phys. Rev. Lett. **65**, 1148 (1990).
- <sup>4</sup>A. Liechtenstein, V. Anisimov, and J. Zaanen, Phys. Rev. B **52**, R5467 (1995).
- <sup>5</sup>P. Wei and Z. Q. Qi, Phys. Rev. B **49**, 10 864 (1994).
- <sup>6</sup>I. Mazin and V. Anisimov, Phys. Rev. B **55**, 12 822 (1997).
- <sup>7</sup>I. Solov'yev, N. Hamada, and K. Terakura, Phys. Rev. B **53**, 7158 (1996).
- <sup>8</sup>J. Perdew, in *Electronic Structure of Solids '91*, edited by P. Ziesche and H. Eschrig (Akademie Verlag, Berlin, 1991), pp. 11-20.
- <sup>9</sup>H. Sawada, N. Hamada, and K. Terakura, Physica B **237-238**, 46 (1997).
- <sup>10</sup>P. Dufek, P. Blaha, V. Sliwko, and K. Schwarz, Phys. Rev. B **49**, 10 170 (1994).
- <sup>11</sup>D. Singh and W. Pickett, Phys. Rev. B **44**, 7715 (1991).
- <sup>12</sup>H. Sawada, N. Hamada, K. Terakura, and T. Asada, Phys. Rev. B **53**, 12 742 (1996).
- <sup>13</sup>D. Ceperley and B. Alder, Phys. Rev. Lett. **45**, 566 (1980).
- <sup>14</sup>J. Perdew and A. Zunger, Phys. Rev. B **23**, 5048 (1981).
- <sup>15</sup>J. Zhu, Ph.D. thesis, University of California at Berkeley, 1990.
- <sup>16</sup>N. Chen, E. Sterer, and I. Silvera, Phys. Rev. Lett. **76**, 1663 (1996).
- <sup>17</sup>P. Loubeyre *et al.*, Nature (London) **383**, 702 (1996).
- <sup>18</sup>S. Weir, A. Mitchell, and W. Nellis, Phys. Rev. Lett. **76**, 1860 (1996).
- <sup>19</sup>W. Kohn and L. Sham, Phys. Rev. A **140**, A1133 (1965).
- <sup>20</sup>R. Dreizler and E. Gross, *Density Functional Theory* (Springer-Verlag, Berlin, 1990).
- <sup>21</sup>J. Perdew *et al.*, Phys. Rev. B **46**, 6671 (1992).
- <sup>22</sup>O. Gunnarsson, M. Jonson, and B. Lundqvist, Phys. Rev. B **20**, 3136 (1979).
- <sup>23</sup>C. Umrigar and X. Gonze, Phys. Rev. A **50**, 3827 (1994).
- <sup>24</sup>C. Umrigar and X. Gonze, in *High Performance Computing and its Applications in the Physical Sciences: Proceedings of the Mardi Gras '93 Conference*, edited by D. A. Browne *et al.* (World Scientific, River Edge, NJ, 1993).
- <sup>25</sup>J. Slater, Phys. Rev. **82**, 538 (1951).
- <sup>26</sup>J. Hubbard, Proc. R. Soc. Sect. A **276**, 238 (1963).
- <sup>27</sup>J. Brandow, Adv. Phys. **26**, 651 (1977).
- <sup>28</sup>N. F. Mott, *Metal Insulator Transistors* (Taylor and Francis, London, 1974).
- <sup>29</sup>N. F. Mott, Proc. Phys. Soc. Sect. A **62**, 416 (1949).
- <sup>30</sup>J. H. Rose, H. Shore, and L. Sander, Phys. Rev. B **21**, 3037 (1980).
- <sup>31</sup>L. Sander, H. Shore, and J. H. Rose, Phys. Rev. B **24**, 4879 (1981).
- <sup>32</sup>B. Min, T. Oguchi, H. Jansen, and A. Freeman, Phys. Rev. B **33**, 324 (1986).
- <sup>33</sup>V. Moruzzi and P. Marcus, Phys. Rev. B **43**, 825 (1991).
- <sup>34</sup>X. W. Wang, J. Zhu, S. G. Louie, and S. Fahy, Phys. Rev. Lett. **65**, 2414 (1990).
- <sup>35</sup>K. Ho, C. Elsässer, C. Chan, and M. Fähnle, J. Phys.: Condens. Matter **4**, 5189 (1992).
- <sup>36</sup>H. J. Monkhorst and J. D. Pack, Phys. Rev. B **13**, 5188 (1976).